separations

MDPI

Article

Economic, Environmental, and Safety Multi-Objective Optimization Design for Separation of Tetrahydrofuran/Methanol/Water Mixture

Mengdie Gao, Qiyu Zhang, Zhehao Jin, Yishan Liu and Yiyang Dai *

School of Chemical Engineering, Sichuan University, Chengdu 610065, China; 18200246045@163.com (M.G.); 2023141490337@stu.scu.edu.cn (Q.Z.); jzh913281@163.com (Z.J.); liuyishansusie@163.com (Y.L.)
* Correspondence: daiyy@scu.edu.cn

Abstract

Tetrahydrofuran (THF) and methanol (MeOH) are widely used as organic solvents in chemical, pharmaceutical, and other industrial fields. The wastewater from producing 1,4-butanediol contains THF, MeOH, and water ternary azeotropic mixture. In this study, to protect the environment and improve economic feasibility, THF and MeOH from the wastewater must be recovered. Triple-column extractive distillation (TED), pressure-swing azeotropic distillation (PSAD) and reactive extractive dividing-wall column (REDWC) are introduced to separate this ternary system, and the NSGA-III algorithm is introduced to optimize the processes, taking the total annual cost (TAC), CO_2 emissions, and process route index (PRI) as objective functions. The results indicate that in comparison with TED process, TAC of PSAD and REDWC is reduced by 29.92% and 24.25%, respectively, and CO_2 emissions decreased by 18.01% and 25.13%, while PRI increased by 150.25% and 100.50%. This study can provide an insight for the design of ternary azeotropic system separation.

Keywords: ternary azeotropic system; NSGA-III algorithm; safety index; mixture separation design

Academic Editor: Ronald Beckett

Received: 18 August 2025
Revised: 13 September 2025
Accepted: 19 September 2025
Published: 21 September 2025

Citation: Gao, M.; Zhang, Q.; Jin, Z.; Liu, Y.; Dai, Y. Economic, Environmental, and Safety Multi-Objective Optimization Design for Separation of Tetrahydrofuran/Methanol/Water Mixture. *Separations* **2025**, *12*, 255. https://doi.org/10.3390/separations12090255

Correction Statement: This article has been republished with a minor change. The change does not affect the scientific content of the article and further details are available within the backmatter of the website version of this article.

1. Introduction

Tetrahydrofuran (THF) and methanol (MeOH) are widely used as organic solvents in chemical, pharmaceutical, and other industrial fields [1,2]. The production process of 1,4-butanediol generates significant quantities of wastewater containing THF, MeOH, and water [3]. To comply with environmental regulations and prevent resource waste, THF and MeOH need to be retrieved from the wastewater. However, in the THF/methanol/water system, there are two azeotropic systems, making it difficult to be separated through ordinary distillation. Thus, special distillations must be used to meet the separation demand, such as extractive distillation (ED) [4], reactive distillation (RD) [5] and pressure-swing distillation (PSD) [6]. Generally, it has previously been observed that the design of ternary azeotropic separation poses greater technical challenges than that of binary azeotropic separation [7].

Extractive distillation (ED) is a widely used method in separating multiple azeotropes by adding a mass separating agent called entrainer. Cui et al. [8] explored an efficient extractive distillation method for the separation of ethyl acetate (EtAc)/isopropanol (IPA)/water system through COSMO-SAC model. Jin et al. [9] investigated a triple-column extractive

distillation (TED) containing a concentration column and a triple-column extractive distillation that contains extractive distillation, a solvent recovery column and a conventional distillation column for separating THF/MeOH/the water system.

Pressure-swing distillation (PSD) can vary in pressure to alter the composition of the azeotrope to separate azeotropes. A greater shift in azeotropic composition under different pressure yields better economic feasibility [3]. Pressure-swing azeotropic distillation can be used when the azeotropic composition exceeds 5% [10]. Jin et al. [9] used PSAD to separate the THF/MeOH/water mixture, which saved 5.75% of the total annual cost (TAC) and reduced 29.1% of CO_2 emissions compared with triple-column extractive distillation.

Reactive distillation (RD) is a common intensification technology that breaks the azeotropic system to achieve the separation goal through chemical reaction and distillation, and it can be further designed into a double-column reactive-extractive distillation column (DRED). Yan et al. [11] studied the recovery and utilization of the benzene/isopropanol/water ternary wastewater through TED and DRED. The optimized DRED achieved a 39.03% reduction in TAC and a 68.42% decrease in CO_2 emissions compared to TED. Meanwhile, dividing the wall column (DWC) represents a process intensification technology, by integrating two conventional columns into a single unit. Zhang et al. [12] have found that compared to traditional distillation sequences, TAC can be reduced by 8.37% in DWC. Furthermore, DWC can be integrated into a reactive-extractive dividing-wall column (REDWC) with DRED, which enables the separation of ternary azeotropes completed in a single column. Huang et al. [13] reported that when compared with TED, REDWC achieves a 46.01% reduction in TAC and a 68.27% reduction in CO_2 emissions.

With the TAC and CO_2 emissions as the main optimization objectives when optimizing the system [14], however, these studies often overlook safety factors, which are crucial in process design. The process route index (PRI) is used as an indicator of safety factors in this work [15], which include density, pressure, flammability, and heating value. It is proposed to quantify inherent safety and address the identified issues, aiming to comprehensively quantify the inherent safety level of a process route by overcoming the limitations of conventional indices [16]. Meanwhile, it is necessary to optimize the operating parameters of the designed process, but the built-in optimization method in Aspen Plus such as sensitivity analysis easily falls into a local optimal solution. Thus, it is essential to discover a global optimization approach. Due to the high nonlinearity of the process, a multi-objective evolutionary algorithm such as non-dominated sorting genetic algorithm II (NSGA-II) [17] and non-dominated sorting genetic algorithm III (NSGA-III) [18] is applied to separate the ternary azeotropic system in this work. However, when the number of objectives exceeds two, NSGA-III outperforms NSGA-II. Thus, NSGA-III is employed to optimize all the processes in this work.

Above all, this work will be organized in the following way. Through the thermodynamic analysis, three processes including TED, PSAD and REDWC are designed for THF/MeOH/water ternary mixture separation. Subsequently, the NSGA-III algorithm is utilized to optimize the economic, environmental, and safety index of these processes, with the triple objectives of reducing TAC, lowering CO_2 emissions and decreasing PRI. Ultimately, the Pareto front is obtained through the algorithm, with the optimized results of the three processes being the point of the Pareto curve.

2. Methodology

2.1. Thermodynamic Analysis

The flow rate of the wastewater is set as 2985.04 kg h^{-1}, containing 21.62% THF, 60.34% methanol and 18.04% water, while the purity of the final product is set as 99.5%THF, 99.55%MeOH and 99%water. Meanwhile, the NRTL model is applicable to the system containing alcohols and various hydroxyl-functionalized components [19]. Therefore, all the process simulations are performed with Aspen Plus V11, where the built-in NRTL model is employed to characterize and predict the thermodynamic behavior of the wastewater, and the missing binary parameters were estimated with the UNIFAC model. [20] The built-in binary interaction parameters of the system are shown in Table S1, which is sourced from the NRTL-1 library of Aspen Plus V11. Figure 1a illustrates the two minimum-boiling binary azeotropes formed in the THF/MeOH/water system: THF/MeOH and THF/water. Additionally, the distillation boundary divides the diagram into two parts so that conventional distillation cannot cross the distillation boundary [21]. Therefore, it is essential to develop advanced separation methods to fulfill the separation demands.

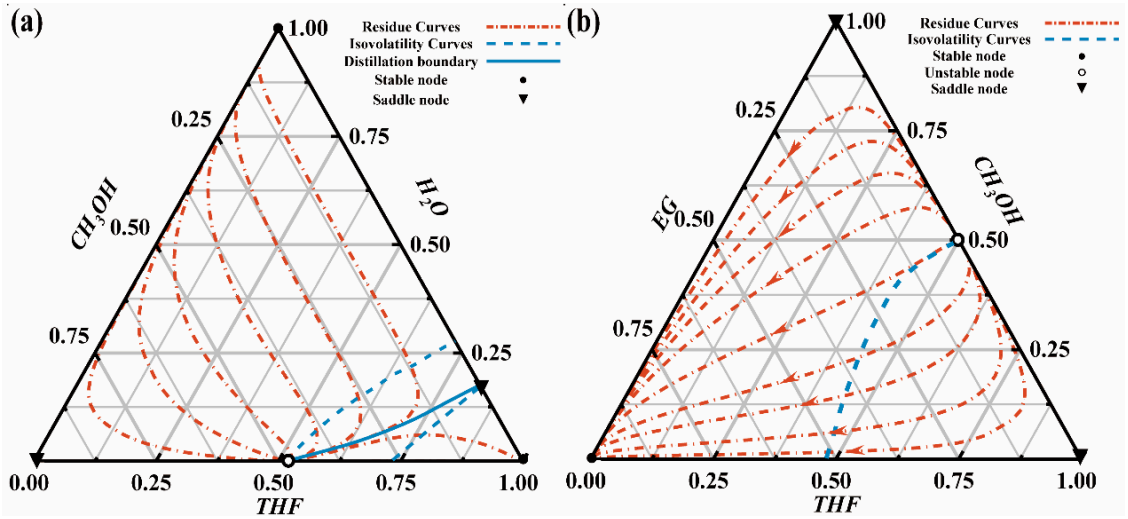

Figure 1. Ternary phase diagram for (**a**) THF/methanol/water system and (**b**) THF/methanol/EG system.

As THF and MeOH are the expected products, the aqueous azeotrope complicates the separation process. Therefore, EO is introduced to consume water to simplify the difficulty of the process. Huang et al. introduced the kinetics of EO hydration to separate ethyl acetate/isopropanol/water, which is also used in this work [11]. The reaction equation and kinetics of EO hydration reaction can be found in Equation (1) and Equation (2), in which x_{EO} and x_{water} represent the mole fraction of EO and water, respectively. According to the hydration reaction, the mole flow rate of the EO feed and the water in the wastewater is at the ratio of 1:1 [9]. EG generated from the reaction can also be used as entrainer to break the THF/MeOH azeotrope, which is shown in Figure 1b [22].

$$EO + H_2O \rightarrow EG \quad (1)$$

$$r\left(kmol{\cdot}m^{-3}\,h^{-1}\right) = 2.8 \times 10^{13} \exp\left[-\frac{71.7}{T}\right] x_{EO}\, x_{water} \quad (2)$$

2.2. Conceptual Design

2.2.1. Triple-Column Extractive Distillation (TED) Process

As shown in Figure 2, the process can be divided into three parts: the extractive distillation column (ED), the conventional distillation column (CD) and the solvent recovery column (SDR). EG and the wastewater are introduced into ED from the upper and intermediate parts, respectively, where MeOH is extracted from the wastewater into EG. The qualified THF is obtained as distillate, while the ED bottom stream simultaneously enters CD. In CD, the distillation process effectively separates the light component, MeOH, and the heavy components, EG and water, achieving the required purity standards. Then, EG is carried out from the bottom of SDR for recycling while the qualified water is obtained as distillate. As EG is partially lost during the distillation process, replenishment is necessary to ensure the purities of the THF and MeOH products meet the required standards.

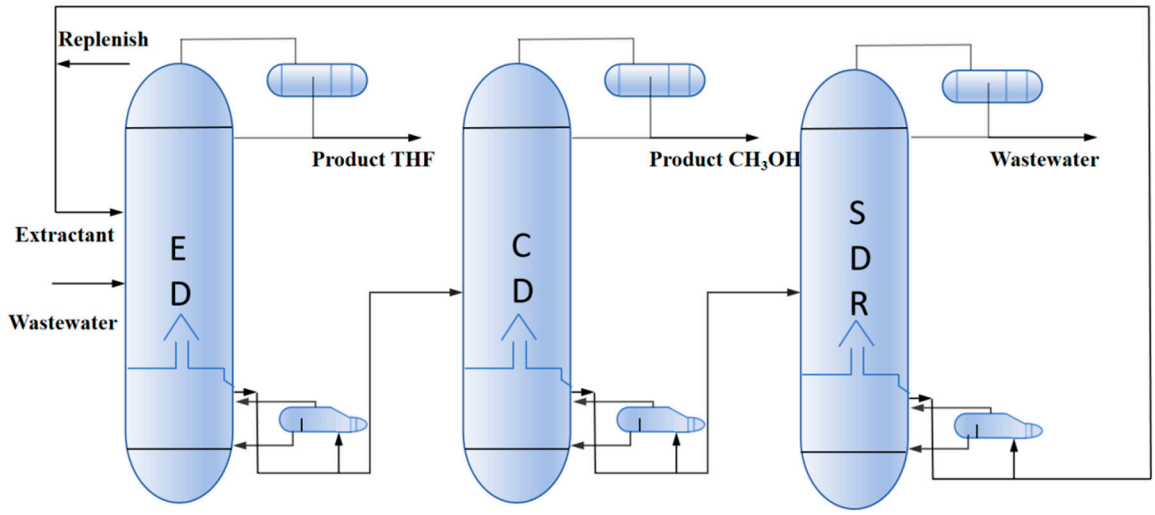

Figure 2. Triple-column extractive distillation process.

2.2.2. Pressure-Swing Azeotropic Distillation (PSAD) Process

Since the main difficulty of separation lies within THF and methanol, the choice of pressure should account for their influence. Based on the T-XY diagram of THF and MeOH in Figure 3, the THF/MeOH azeotrope shows certain deviations at 0.1 Mpa and 0.6 Mpa. At 0.1 Mpa, the mass fraction of THF is approximately 0.48, while at 0.6 Mpa, it is around 0.69. The azeotropic difference between the two pressures exceeds 5%, allowing for 0.1 Mpa and 0.6 Mpa to be used as the pressure of the low-pressure column (LP) and the high-pressure column (HP), respectively, to achieve the desired separation.

Figure 4 shows the process of PSAD, which contains three parts: LP, HP, and CD. The wastewater is fed into the intermediate of the LP, and the distillate containing THF and MeOH is sent to the middle part of HP, while the bottom stream is fed into CD. The bottom of HP produces the purified THF, while the remaining THF–methanol mixture returns to LP for further separation. Meanwhile, MeOH and water are separated in the CD, with high-purity MeOH obtained as distillate and wastewater discharged from the bottom.

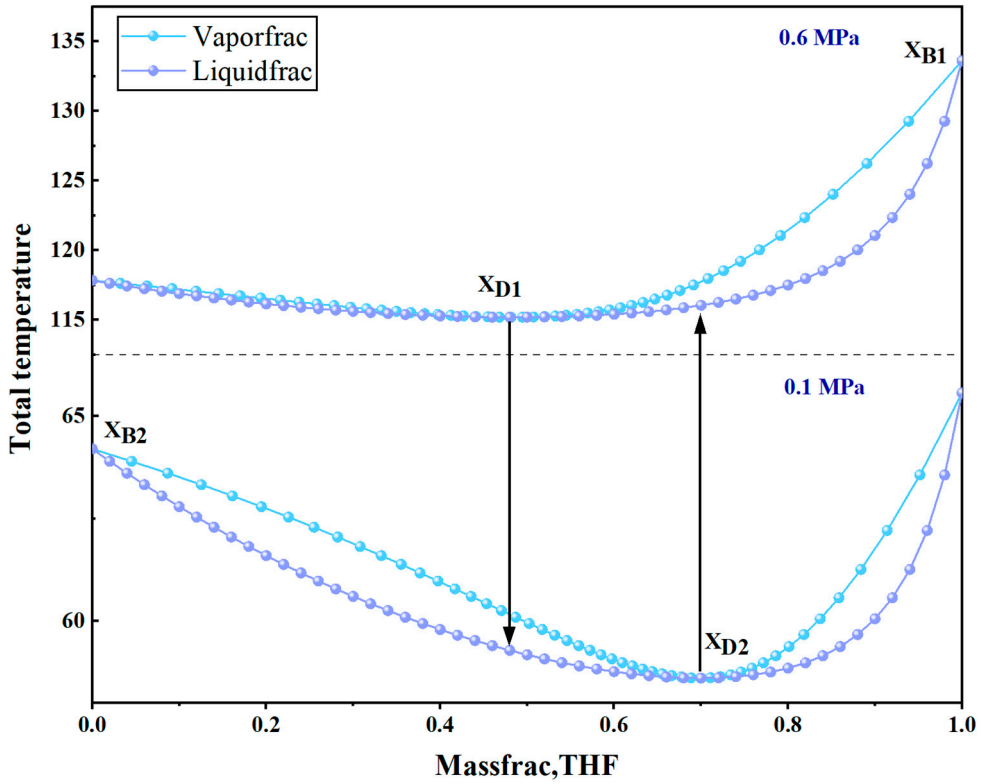

Figure 3. T-XY diagram of the pressure-swing azeotropic distillation for separating the minimum-boiling azeotropic mixture.

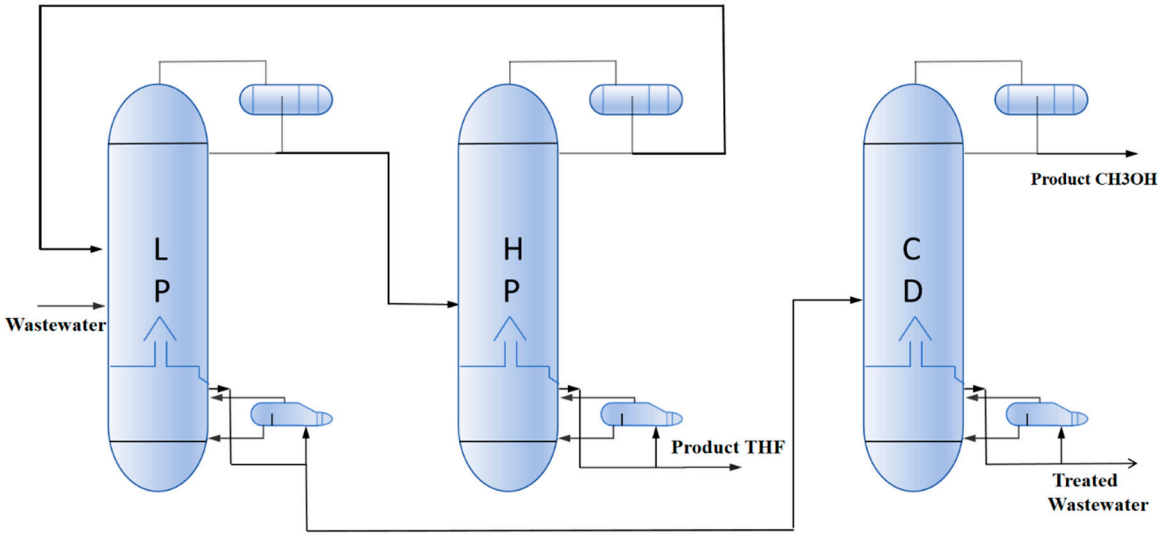

Figure 4. Pressure-swing azeotropic distillation process.

2.2.3. Reactive-Extractive Dividing Wall Column (REDWC)

In the REDWC process, all the operations such as the EO hydration reaction, the separation of wastewater, and the solvent recovery are completed in one column, with only one reboiler, reducing TAC and CO_2 emissions. The column is divided into two parts: the main column (MC) serves as the feed inlet and reaction zone, while the side column (SC) functions as the MeOH product recovery section [23]. As shown in Figure 5, the entrainer EG, the materials, and EO are fed into the column from the upper part, the upper-middle part and the middle part, respectively. The EO hydration reaction takes place at the middle part of MC, generating the entrainer EG. Meanwhile, the vapor stream from the column base is distributed between MC and SC to facilitate the mass transfer in vapor–liquid

interfaces. The qualified THF is extracted from MC, and the light MeOH is distillated in SC. High-purity EG is obtained as the bottom product, which is partially recycled to MC after cooling and is still used as entrainer.

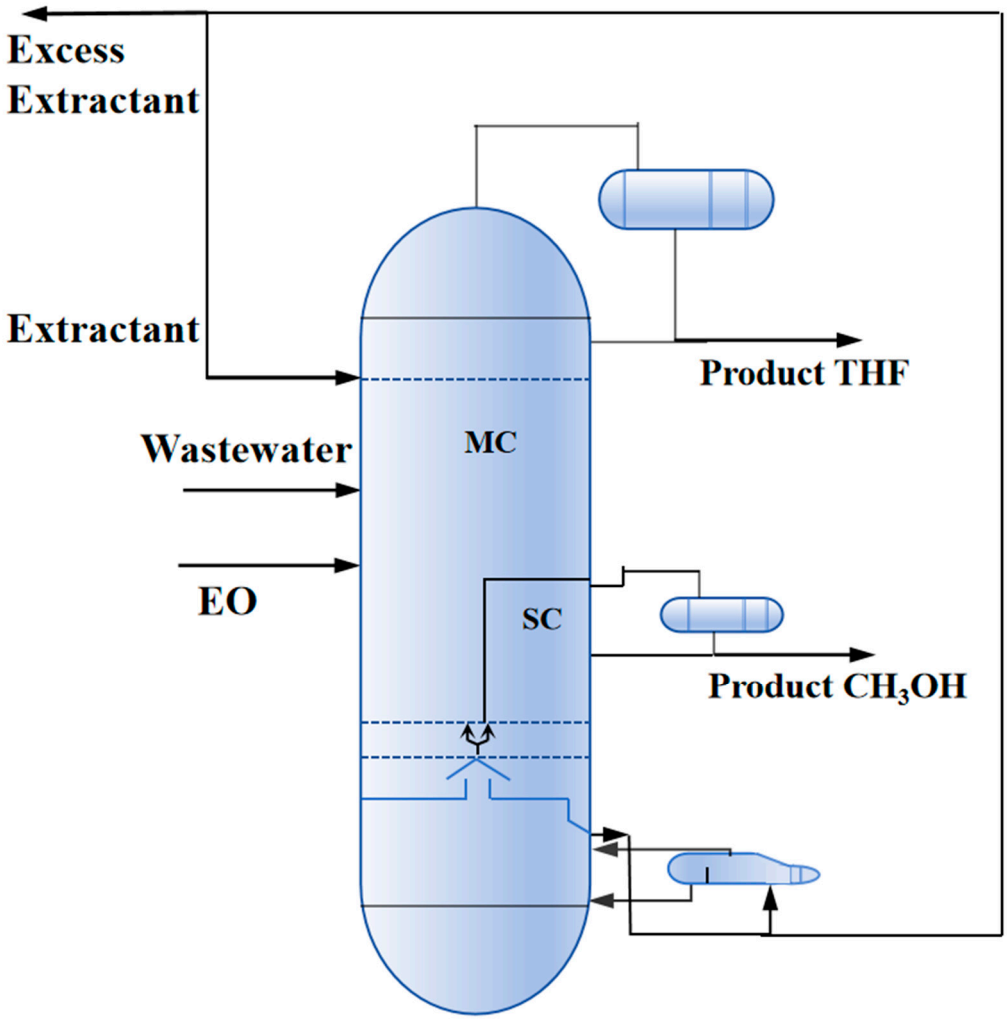

Figure 5. Reactive-extractive dividing wall column process.

2.3. Performance Evaluation

To assess the performance of the three separation methods, we use TAC, CO_2 emissions, and PRI as key performance indicators. More detailed performance evaluation calculations can be found in Table S2.

2.3.1. Economic Index

The total annual cost (*TAC*) is the primary economic evaluation metric, with its calculation formula provided in Equation (3) [24]. The *CAPEX* includes the costs of columns, pumps, reboilers, and condensers, while *OPEX* represents the sum of utility costs. The investment recovery period is established as 3 years. Detailed economic calculation equations are provided in the Supplementary Section S2.

$$TAC = \frac{CAPEX}{Payback\ Period} + OPEX \quad (3)$$

2.3.2. Environmental Index

With the growing importance of environmental concerns, CO_2 emissions have become a key indicator for assessing processes' environmental impact. Using natural gas as the fuel source, it can be calculated in Equation (4).

$$CO_2\ emission\left(\frac{kg}{h}\right) = \frac{Q_{fuel}}{NHV}\cdot\frac{C\%}{100}\cdot\alpha \tag{4}$$

Q_{fuel} stands for the heat duty of fuel consumption (kW), NHV denotes the net heating value (kJ/kg), and C refers to the carbon content; detailed information about the environmental index calculation equations can be found in the Supplementary Section S2.

2.3.3. Safety Index

The process route index (PRI) is an important indicator for safety factors, evaluating the safety of the process through four aspects: density, pressure, flammability, and heating value. The PRI can be calculated by Equation (5) [14].

$$PRI = \frac{(MHV_{average})(MDEN_{average})(P_{average})(COMB_{average})}{10^8} \tag{5}$$

$MHV_{average}$ is the average mass heating value (kJ kg^{-1}); $MDEN_{average}$ is the average fluid density (kg m^{-3}); $P_{average}$ is the average pressure (atm); and $COMB_{average}$ is the average combustibility (%). The detailed information is shown in the Supplementary Section S2.

2.4. Optimization Strategy

It is essential to optimize the process to achieve balanced performance in the aspects of economy, environmental protection, and safety. The specific optimization objective function is shown in Equation (6). Aiming to minimize TAC, CO_2 emissions, and the PRI, NSGA-III is employed to optimize process parameters. Moreover, the purity of the components is considered to be the constraint; therefore, if constraints were not met during optimization, the penalty coefficient was increased to ensure the final solution set satisfied the requirements.

$$\begin{gathered}\min_x[f_1(economy),\ f_2(environment),\ f_3(safety)]\\ s.t.x_{THF} \geq 0.995\\ x_{Methnol} \geq 0.995\\ x_{Water} \geq 0.99\end{gathered} \tag{6}$$

The optimization process involves both integer and real operating parameters. Therefore, the optimization is mathematically modeled as a mixed-integer nonlinear programming formulation. To enhance the convergence speed, a numerical range of optimization variables is necessary, which can be found in Table S4. Throughout the optimization process, the ActiveX interface is used to link Aspen Plus with MATLAB 2024A, employing the NSGA-III [25] algorithm for optimization.

Meanwhile, the key variables exhibit the following influences: An increase in the reflux ratio enhances product purity but raises both CO_2 emissions and PRI. A greater number of stages leads to higher TAC but reduces both CO_2 emissions and PRI. Higher distillate flow rate reduces the purity of the product. An increased entrainer flow rate increases TAC and CO_2 emissions but decreases PRI. Consequently, TAC, CO_2 emissions, and PRI are not positively correlated.

There are seven integer variables to be optimized in TED, namely, the number of trays (N_1, N_2, N_3), the feed stage ($NF_{entrainer}$, NF_{Feed}, NF_1, NF_2) and seven real variables,

namely, the reflux ratio (RR_1, RR_2, RR_3), the flow rates of distillate (DF_1, DF_2, DF_3), and the entrainer flow rate (F_{EG}).

There are six real variables to be optimized in PSAD, namely, the reflux ratio (RR_1, RR_2, RR_3), the flow rates of distillate (DF_1, DF_2), and the bottom product flow rate (BF1), and seven integer variables, namely, the number of trays (N_1, N_2, N_3) and the feed stage (NF_{Reflux}, NF_{Feed}, NF_1, NF_2).

There are seven real variables to be optimized in the REDWC process, namely, the reflux ratio (RR_1, RR_2), the flow rates of distillate (DF_1, DF_2), the flow rate of EG (F_{EG}), the mole liquid holdup (LH) and the vapor flow rate (V_1), and six integer variables, namely, the number of trays (N_1, N_2, N_3) and the feed stage (NF_{EO}, NF_{Feed}, NF_1, NF_2, VF_1).

Meanwhile, Figure 6 shows the optimization steps. Based on NSGA-III, the initial population is generated by MATLAB. Then, the candidate solutions are evaluated through Aspen Plus via ActiveX interface, which returns the performance indicators, including TAC, CO_2 emissions and PRI, under the purity constrains. Each generation iterates through crossover and mutation until the preset criteria is met. The Pareto front is ultimately obtained through the algorithm that effectively balances optimization objectives and the constraints. To obtain more accurate Pareto-optimal solutions, a population size of 200 is used, and the algorithm is iterated for 200 generations. All optimization is performed on a laptop with i9-13900h CPU.

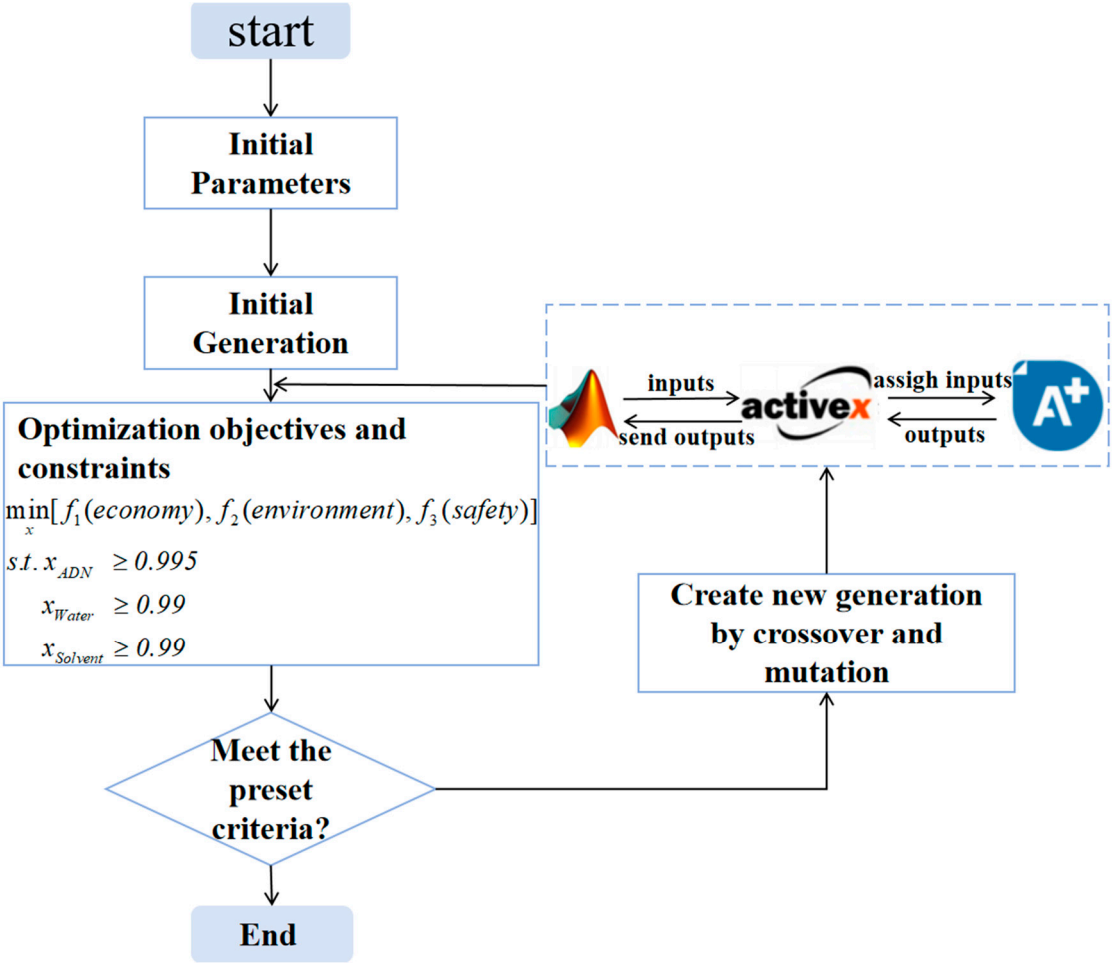

Figure 6. The flowchart of the optimization process.

3. Results and Discussions

3.1. Results of Multi-Objective Optimization

After taking 50 h, 48 h, and 54.5 h for TED, PSAD, and REDWC, respectively, the result of the optimizing process parameters with the NSGA-III algorithm is illustrated in Figure 7. All data from the Pareto front can be found in Table S7.

The Pareto front of RED, PSAD, and REDWC is graphically represented in Figure 7 a–c, respectively, where red triangles denote two key cases in each process, and the detailed parameters are shown in Table 1: the most economical and environmental design, and the safest design, namely Case 1 and Case 2, respectively. Due to the small range of the feasible variables and the complexity of the process, all the shapes of the scattered points are close to the Pareto curve. It is obvious that the value of PRI is inversely proportional to both TAC and CO_2 emissions. The lower the PRI is, the higher TAC and CO_2 emissions are. This occurs because of the reduction in the flow rate of the entrainer, pressure, and reflux ratio will reduce TAC and CO_2 emissions while increasing the PRI. Points enclosed by triangles are further used for an optimal process.

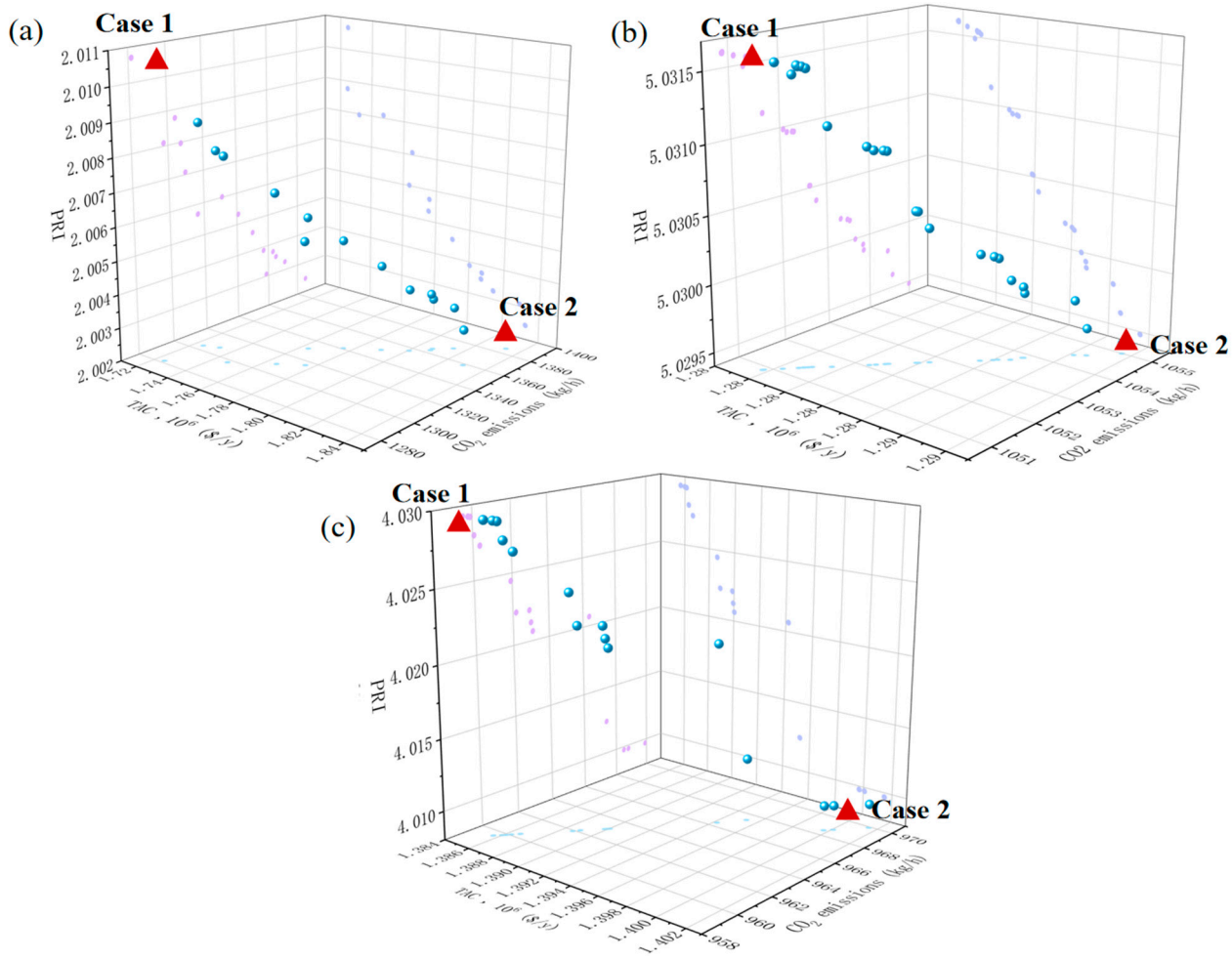

Figure 7. Optimization results of (**a**) TED, (**b**) PSAD and (**c**) REDWC.

Table 1. Detailed design parameters of TED, PSAD and REDWC process.

	TED		PSAD		REDWC	
Variables	**Case 1**	**Case 2**	**Case 1**	**Case 2**	**Case 1**	**Case 2**
N_1	65	62	29	29	65	63
$NF_{Extractant}$	4	3	7	7	3	3
NF_{Feed}	26	28	11	11	21	22
RR	0.7	0.85	1.96	1.99	1.93	2.02
DF_1	644.99	644.75	2072.24	2079.2	642.19	642.2
LH	/	/	/	/	8.41	10
V	/	/	/	/	1848.43	1855
VF	/	/	/	/	53	52
N_2	22	20	21	19	7	6
NF_2	14	12	15	13	/	/
RR_2	0.94	0.95	1.72	1.82	/	/
DF_2	1802.46	1802.01	643.09	643.68	1805.39	1805.68
F_{EG}	/	/	/	/	20,336.75	20,488.57
N_3	21	15	18	18	/	/
NF_3	9	10	14	14	/	/
RR_3	0.65	0.81	1.1	1.1	/	/
DF_3	540.02	539.71	1802.49	1802.42	/	/

3.2. Results of Optimal Processes

Figures 8–10 graphically summarize the optimal parameters of the TED, PSAD, and REDWC processes.

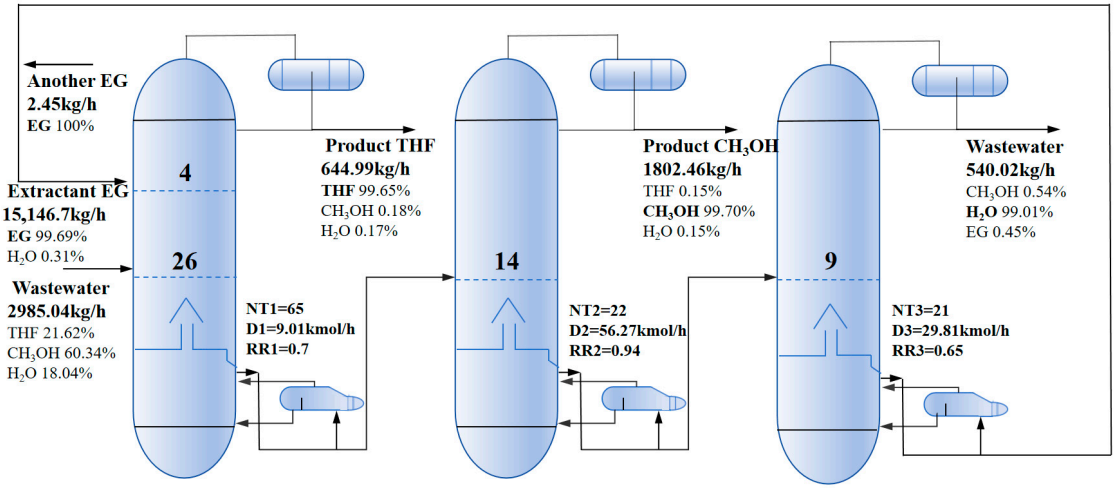

Figure 8. Optimal parameter of TED process.

As shown in Figure 8, EG and the wastewater enter ED at the 4th and 26th stages, respectively, and MeOH is extracted from the wastewater to EG. Consequently, THF is obtained as distillate, with a flow rate of 644.99 kg h^{-1} and a purity of 99.65%. The bottom stream containing MeOH, EG, and water is fed to CD at the 14th stage. Owing to the large boiling point differences among MeOH, EG, and water, MeOH is obtained as distillate with a flow rate of 1802.46 kg h^{-1} and a purity of 99.70%. Then, EG and water enter SDR at the ninth stage, with the treated wastewater discharged and the high-purity EG recycled after cooling. As EG is partially lost during the distillation process, an additional 2.45 kg h^{-1} EG is added with the previous EG as the entrainer.

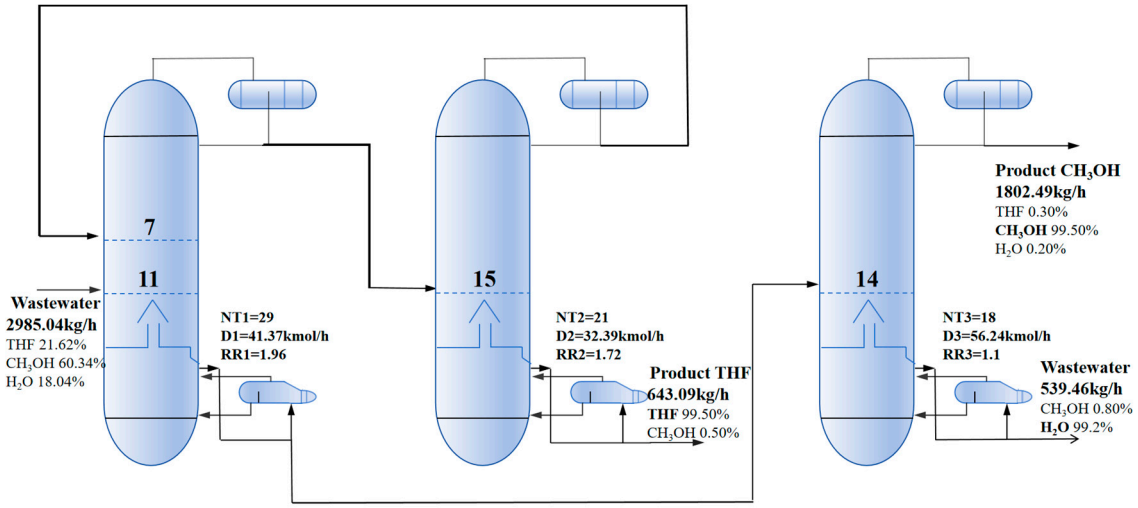

Figure 9. Optimal parameter of PSAD process.

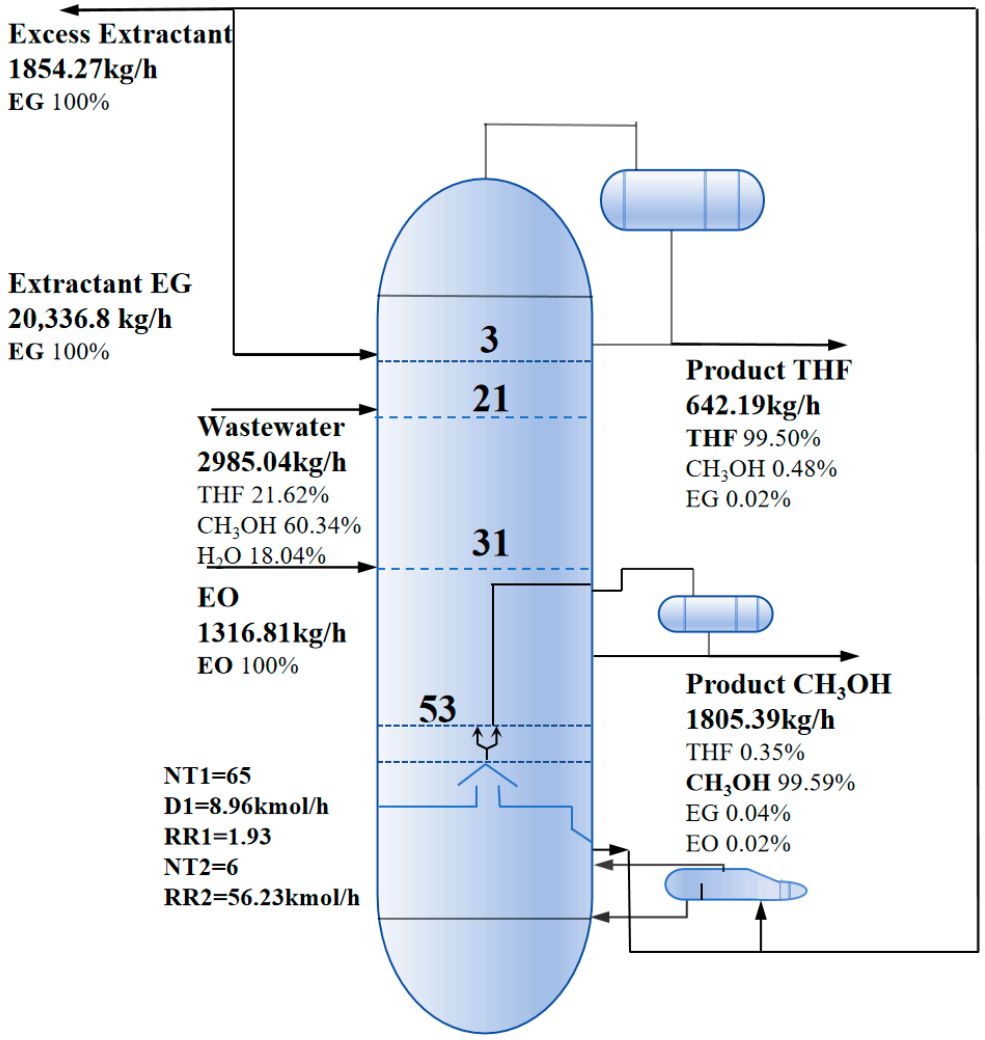

Figure 10. Optimal parameter of REDWC process.

Figure 9 illustrates that the wastewater stream enters LP at the 11th stage. The THF/MeOH azeotrope obtained as distillate is sent to the HP for further separation, while the MeOH/water mixture from the bottom is sent to the CD as feed. In the HP, feed introduced at the 15th stage yields 643.09 kg h^{-1} of THF with a purity of 99.50% at the bottom, while the

distillation stream returns the remaining THF/MeOH azeotrope to LP. In CD, feed enters at the 14th stage and MeOH is obtained as distillate with a flow rate of 1802.49 kg h^{-1} and a purity of 99.50%, and the bottom discharges treated wastewater at 99.2% purity.

Figure 10 shows that wastewater and EO enter the MC at the 21st and 31st stages, respectively, and then the countercurrent contact between EO and water generates EG. Simultaneously, EG fed at the third stage extracts MeOH from the wastewater. As a result, THF is obtained as distillate in the MC with a flow rate of 642.19 kg h^{-1} and a purity of 99.50%. In addition, 1848.43 kg h^{-1} of vapor steam from the MC bottom is directed to SC, where MeOH is obtained as distillate with a flow rate of 1805.39 kg h^{-1} and a purity of 99.59%. To save resources, EG obtained as the bottom product is recycled after cooling. To maintain liquid balance, 1854.27 kg h^{-1} of EG is withdrawn during recycling.

3.3. Economic, Environmental and Safety Evaluation

Figure 11 graphically summarizes the TAC, CO_2 emission, and PRI values for all three different processes in this work. The TACs of TED, PSAD, and REDWC are 1.83 × 10^6 \$, 1.28 × 10^6 \$, and 1.38 × 10^6 \$ each year, respectively, while the CO_2 emissions of these processes are 1358.53, 1053.84, and 969.80, respectively. Compared with TED, PSAD and REDWC are economically and environmentally attractive, which reduced TAC by 29.73% and 23.46%, and CO_2 emission by 22.43% and 28.69%, respectively. This occurs because for the PSAD process, the pressure swing replaces the entrainer addition, reducing the operating cost of both the condenser and reboiler. For the REDWC process, integrating all operations into a single column reduces the capital cost and the operating cost of the reboiler. Moreover, the heat that the EO hydration reaction generates can also reduce the heat of the reboiler. Since identical fuel was utilized across all processes, CO_2 emissions are only determined to be the duty of the reboiler. Consequently, TAC and CO_2 emissions of PSAD and REDWC are more significantly reduced than that of TED.

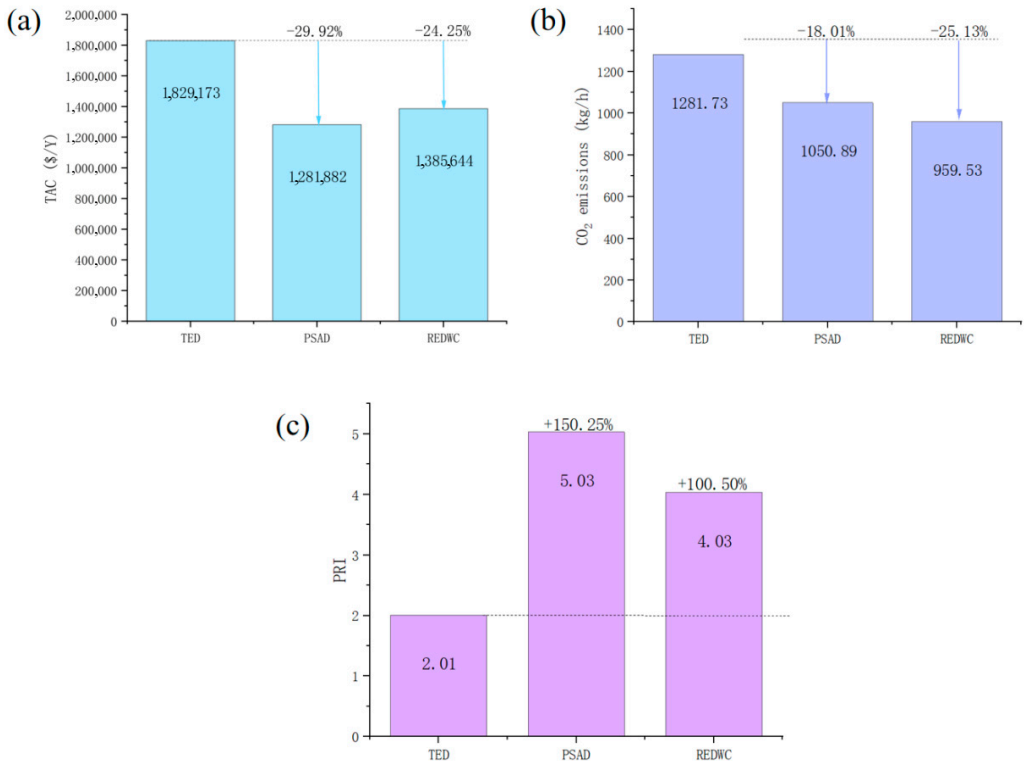

Figure 11. Performance evaluation from the aspects of (**a**) economy, (**b**) environment, and (**c**) safety.

However, regarding PRI, PSAD shows the highest value of 5.03, while TED and REDWC have values of 2.01 and 4.03, respectively. The reason for this is that in the PSAD process, the value of pressure is more than twice as high as TED and REDWC, while in REDWC, the introduction of EO enhances the value of combustibility. Therefore, TED is the safest process among the three.

4. Conclusions

In this paper, TED, PSAD, and REDWC are proposed to separate THF/MeOH/water ternary azeotropes to achieve a sustainable process. With the goal of achieving an economic, environmental, and safe process, NSGA-III is employed to optimize. Moreover, the introduction of the EG and EO hydration reaction reduces the complexity of the process. The result shows that compared with TED, PSAD and REDWC are economically and environmentally attractive, which reduced TAC by 29.92% and 24.25%, and CO_2 emissions by 18.01% and 25.13%, respectively. But regarding PRI, PSAD and REDWC increased by 150.25% and 100.50%, respectively.

This work can provide certain ideas for the design of other separation systems. However, the applicability of the proposed separation is currently restricted to wastewater treatment scenarios. In addition, the exergy can also be considered for analysis, which will be performed in further work.

Supplementary Materials: The following supporting information can be downloaded at: https://www.mdpi.com/article/10.3390/separations12090255/s1, Section S1: Process modeling; Table S1: The built-in binary interaction parameters of the work. Section S2: Performance indices; Table S2: Utilities cost in the TAC calculation; Table S3: Flammability calculation of THF, methanol and EG; Section S3: Variable range; Table S4: Variation range of decision variables for TED; Table S5: Variation range of decision variables for PASD; Table S6: Variation range of decision variables for REDWC; Section S4: Algorithms comparison; Table S7: The detailed data of the TED, PSAD and REDWC with NSGA-III algorithms optimization [26–29].

Author Contributions: M.G.: Investigation, Resources, Formal analysis, Visualization. Writing—original draft, Writing—review and editing. Q.Z.: Funding acquisition, Software, Formal analysis, Project administration, Supervision. Z.J.: Supervision, Methodology, Project administration. Y.L.: Validation, Visualization, Data curation. Y.D.: Supervision, Conceptualization, Project administration. All authors have read and agreed to the published version of the manuscript.

Funding: This research was funded by Sichuan Science and Technology Program grant number 2021YFH0116.

Data Availability Statement: The original contributions presented in this study are included in the article/supplementary material. Further inquiries can be directed to the corresponding author.

Conflicts of Interest: The authors declare that they have no known competing financial interests or personal relationships that could have appeared to influence the work reported in this paper.

Abbreviations

THF	tetrahydrofuran
CC	conventional column
EG	ethylene glycol
MeOH	methanol
RD	reactive distillation
EtAC	ethyl acetate
IPA	isopropanol
TED	triple-column extractive distillation
DMSO	dimethyl sulfoxide

ED	extractive distillation
CD	conventional distillation
PSD	pressure-swing distillation
PSAD	pressure-swing azeotropic distillation
SDR	solvent recovery column
LP	low-pressure column
HP	high-pressure column
DRED	reactive-extractive distillation column
DWC	dividing wall column
REDWC	reactive-extractive dividing wall column
NSGA-II	non-dominated sorting genetic algorithm II
NSGA-III	non-dominated sorting genetic algorithm III
MC	main column
SC	side column
TAC	total annual cost
PRI	The process route index
N	stage
NF	feed stage
RR	reflux ratio
DF	distillate flow rate
FEG	entrainer content

References

1. Zhao, N.; Yang, J.; Ai, T.; Wang, J. From Methanol to Power: Energy, Economic and Life-Cycle Assessments of Several Pathways. *J. Clean. Prod.* **2025**, *486*, 144501. [CrossRef]
2. Chen, Z.; Du, Z.; Wang, T.; Chen, L. The Impact of THF in Ether-Based Electrolytes for Lithium-Sulfur Battery. *Ionics* **2025**, *31*, 1377–1388. [CrossRef]
3. Wang, Z.; Luo, C.; Wang, B.; Lai, T.; Hong, Y.; Gao, G. Synergistic Catalysis of Sulfate Ionic Liquids and FeCl3 for the Dehydration of 1, 4-Butanediol to Tetrahydrofuran. *Fuel* **2024**, *363*, 130806. [CrossRef]
4. Liu, C.; Karagoz, A.; Alqusair, O.; Ma, Y.; Xiao, X.; Li, J. Design of Hybrid Reactive-Extractive Distillation for Separation of Azeotropic Ternary Mixture Using a Systematic Optimization Framework. *Sep. Purif. Technol.* **2025**, *369*, 132805. [CrossRef]
5. Serpas, C.G.; Samborskaya, M.; Mityanina, O. Parametric Optimization of a Reactive Distillation Column for the Ethyl Tert-Butyl Ether Production. *Period. Polytech. Chem. Eng.* **2024**, *68*, 116–123. [CrossRef]
6. Dai, T.; Li, J.; Wang, H.; Zhang, R.; Ye, Q. Sustainable Recovery of Benzene and Tert-Butanol from Wastewater Using Energy-Efficient Heterogeneous Azeotropic Pressure-Swing Distillation with Multi-Objective Optimization. *Process Saf. Environ. Prot.* **2025**, *200*, 107317. [CrossRef]
7. Zhao, L.; Lyu, X.; Wang, W.; Shan, J.; Qiu, T. Comparison of Heterogeneous Azeotropic Distillation and Extractive Distillation Methods for Ternary Azeotrope Ethanol/Toluene/Water Separation. *Comput. Chem. Eng.* **2017**, *100*, 27–37. [CrossRef]
8. Cui, P.; Zhao, F.; Liu, X.; Shen, Y.; Li, S.; Meng, D.; Zhu, Z.; Ma, Y.; Wang, Y. Sustainable Wastewater Treatment via PV-Distillation Hybrid Process for the Separation of Ethyl Acetate/Isopropanol/Water. *Sep. Purif. Technol.* **2021**, *257*, 117919. [CrossRef]
9. Jin, Z.; Liu, H.; Dai, Z.; Dai, Y. Investigation on Energy-Saving Distillation for Separating Tetrahydrofuran/Methanol/Water Ternary Azeotropic System. *J. Clean. Prod.* **2024**, *441*, 140899. [CrossRef]
10. Modla, G.; Lang, P. Separation of an Acetone−Methanol Mixture by Pressure-Swing Batch Distillation in a Double-Column System with and without Thermal Integration. *Ind. Eng. Chem. Res.* **2010**, *49*, 3785–3793. [CrossRef]
11. Yan, J.; Liu, J.; Ren, J.; Wu, Y.; Li, X.; Sun, T.; Sun, L. Design and Multi-Objective Optimization of Hybrid Reactive-Extractive Distillation Process for Separating Wastewater Containing Benzene and Isopropanol. *Sep. Purif. Technol.* **2022**, *290*, 120915. [CrossRef]
12. Zhang, X.; Zhu, J.; Zhou, C.; Cao, Q.; Gao, Y.; Li, X.; Hou, Y.; Zhao, W.; Xiang, S.; Wang, L. Designing of Dividing Wall Columns and Triple-Effect Evaporators for Energy-Saving Separation of Glycol (EG+ DEG+ TEG) and Water: An Integrated Approach Considering Energy, Exergy, Economic, and Environmental Analyses. *Sep. Purif. Technol.* **2025**, *373*, 133578. [CrossRef]
13. Huang, J.; Zhang, Q.; Liu, C.; Yin, T.; Xiang, W. Optimal Design of the Ternary Azeotrope Separation Process Assisted by Reactive-Extractive Distillation for Ethyl Acetate/Isopropanol/Water. *Sep. Purif. Technol.* **2023**, *306*, 122708. [CrossRef]

14. Yin, T.; Zhang, Q.; Chen, Y.; Liu, C.; Xiang, W. Process Design and Optimization of the Reactive-Extractive Distillation Process Assisted with Reaction Heat Recovery via Side Vapor Recompression for the Separation of Water-Containing Ternary Azeotropic Mixture. *Process Saf. Environ. Prot.* **2024**, *184*, 1041–1056. [CrossRef]
15. Yang, A.; Kong, Z.Y.; Sun, S.; Sunarso, J.; Ren, J.; Shen, W. Design and Multiobjective Optimization of a Novel Double Extractive Dividing Wall Column with a Side Reboiler Scheme for the Recovery of Ethyl Acetate and Methanol from Wastewater. *Ind. Eng. Chem. Res.* **2023**, *62*, 18591–18602. [CrossRef]
16. Leong, C.T.; Shariff, A.M. Process Route Index (PRI) to Assess Level of Explosiveness for Inherent Safety Quantification. *J. Loss Prev. Process Ind.* **2009**, *22*, 216–221. [CrossRef]
17. Sharma, D.; Vasanthi, D.R.; Reddy, S.G.K.; Rao, M. NSGA-RM: NSGA-II Evolved Performance Optimized Non-Homogeneous Recursive Polynomial Multiplier Architectures. In Proceedings of the 2025 38th International Conference on VLSI Design and 2024 23rd International Conference on Embedded Systems (VLSID), Bangalore, India, 4–8 January 2025; IEEE: New York, NY, USA, 2025; pp. 121–126.
18. Wietheger, S.; Doerr, B. A Mathematical Runtime Analysis of the Non-Dominated Sorting Genetic Algorithm III (NSGA-III). In Proceedings of the Genetic and Evolutionary Computation Conference Companion, Melbourne, Australia, 14–18 July 2024; ACM: New York, NY, USA, 2024; pp. 63–64.
19. Bala, A.M.; Liu, R.; Peereboom, L.; Lira, C.T. Applications of an Association Activity Coefficient Model, NRTL-PA, to Alcohol-Containing Mixtures. *Ind. Eng. Chem. Res.* **2022**, *61*, 15603–15619. [CrossRef]
20. Zhang, Y.-R.; Wu, T.-W.; Chien, I.-L. Intensified Hybrid Reactive-Extractive Distillation Process for the Separation of Water-Containing Ternary Mixtures. *Sep. Purif. Technol.* **2021**, *279*, 119712. [CrossRef]
21. Frolkova, A.V. Structural Analysis of Phase Diagram and Assessment of Possibility for Distillation of Multicomponent Mixtures. *Theor. Found. Chem. Eng.* **2024**, *58*, 1017–1026. [CrossRef]
22. Tavan, Y.; Hosseini, S.H. A Novel Integrated Process to Break the Ethanol/Water Azeotrope Using Reactive Distillation–Part I: Parametric Study. *Sep. Purif. Technol.* **2013**, *118*, 455–462. [CrossRef]
23. Tavan, Y.; Behbahani, R.M.; Hosseini, S.H. A Novel Intensified Reactive Distillation Process to Produce Pure Ethyl Acetate in One Column—Part I: Parametric Study. *Chem. Eng. Process. Process Intensif.* **2013**, *73*, 81–86. [CrossRef]
24. Pandit, S.R.; Jana, A.K. Transforming Conventional Distillation Sequence to Dividing Wall Column: Minimizing Cost, Energy Usage and Environmental Impact through Genetic Algorithm. *Sep. Purif. Technol.* **2022**, *297*, 121437. [CrossRef]
25. Li, E.; Dai, X.; Jia, B. Multi-Dimensional Classification via NSGA-III Algorithm and Sparse Label Encoding. In Proceedings of the 2024 8th International Conference on Electronic Information Technology and Computer Engineering, Haikou, China, 18–20 October 2024; ACM: New York, NY, USA, 2024; pp. 120–128.
26. Parhi, S.S.; Rangaiah, G.P.; Jana, A.K. Multi-Objective Optimization of Vapor Recompressed Distillation Column in Batch Processing: Improving Energy and Cost Savings. *Appl. Therm. Eng.* **2019**, *150*, 1273–1296. [CrossRef]
27. Luyben, W.L. Comparison of Extractive Distillation and Pressure-Swing Distillation for Acetone/Chloroform Separation. *Comput. Chem. Eng.* **2013**, *50*, 1–7. [CrossRef]
28. Shariff, A.M.; Leong, C.T.; Zaini, D. Using Process Stream Index (PSI) to Assess Inherent Safety Level during Preliminary Design Stage. *Saf. Sci.* **2012**, *50*, 1098–1103. [CrossRef]
29. Aurangzeb, M.; Jana, A.K. Double-Partitioned Dividing Wall Column for a Multicomponent Azeotropic System. *Sep. Purif. Technol.* **2019**, *219*, 33–46. [CrossRef]